

# An Accumulation-based, Closed-loop Scheme for Expected Minimum Rate and Weighted Rate Services

David Harrison<sup>†</sup>, Yong Xia, Shivkumar Kalyanaraman, Arvind Venkatesan<sup>†</sup>

<sup>†</sup>CS and ECSE Departments, Rensselaer Polytechnic Institute, Troy, NY 12180, USA

Corresponding email: shivkuma@ecse.rpi.edu

**Abstract**—Traditionally QoS capabilities have been constructed out of open-loop building blocks such as packet schedulers and traffic conditioners. In this paper, we consider *closed-loop* techniques to achieve a range of service differentiation capabilities. We use an accumulation-based congestion control scheme [31] as a data-plane building block to provide an *expected minimum rate* service that is similar to ATM ABR, Frame Relay CIR/PIR and DiffServ assured service and a *weighted rate* service that achieves a significantly larger range than the loss-based approaches that extend TCP [9] [25]. The central theme is to allocate router buffer space among competing flows in a *distributed* manner to meet the rate differentiation objectives. Because both services are provided using the congestion control mechanisms, they are meaningful in steady state and can be modeled as moving the equilibrium in Kelly’s nonlinear optimization framework [16]. This scheme does not require admission control; instead, it degrades to a well-defined, policy-controlled bandwidth allocation during oversubscription. It does not require Active Queue Management (AQM) at bottlenecks with sufficient buffer. However, with AQM, we achieve near zero queue with high utilization at the congested routers. We use ns-2 simulations and Linux kernel implementation experiments to demonstrate the performance of the services. Some practical issues and open questions are also discussed.

**Index Terms**—Quality of Service, Congestion Control, Closed-Loop Mechanisms.

## I. INTRODUCTION

As the Internet evolves as a telecommunication infrastructure, its best-effort service model must be augmented to provide better quality of service (QoS) to support more demanding application requirements. For example, researchers have developed the Integrated Service (IntServ) architecture [5] to provide bandwidth and delay guaranteed services and the Differentiated Service (DiffServ) architecture [4] for service differentiation. Both architectures place their service building blocks inside the network. Trying to move some functionality from the network core toward the network edges or even the

end hosts, this paper proposes the use of accumulation-based, closed-loop congestion control mechanisms as a data-plane building block to provide expected minimum rate and weighted rate services.

The Expected Minimum Rate (EMR) refers to a service that offers a minimum contracted rate assurance plus a proportionally fair share of the remaining available capacity. It is conceptually similar to the ATM ABR Minimum Cell Rate (MCR) [2] and the Frame Relay CIR/PIR that guarantees (through admission control) a Committed Information Rate (CIR) and can burst up to a Peak Information Rate (PIR) [12]. EMR service is also similar to the DiffServ assured service [4], though the latter has multiple classes and drop precedences within each class. ATM ABR MCR, Frame Relay CIR/PIR and DiffServ assured services are realized using open-loop building blocks, such as packet scheduling and traffic conditioning [10] [27].

The weighted rate service (WRS) building block provides weighted bandwidth differentiation among flows that share the same path. We demonstrate that our mechanisms achieve a wider range of weights than the loss-based bandwidth differentiation approaches using TCP [15] [9] [25].

We develop concrete service building blocks based upon our prior work on a family of Accumulation-based Congestion Control (ACC) schemes. ACC uses accumulation, the buffered packets of a flow inside the network, as a congestion measure [31]. An ACC control loop measures its accumulation and adjusts its sending window to keep the accumulation around a target value. In [31] we showed that ACC achieves weighted proportional fairness and has an equilibrium decided by the target accumulations. Our service building blocks map a target rate allocation onto target accumulations. One key concern is that ACC over a network of FIFO queues inherently implies that the bottleneck routers build physical queues, and thus the range of services is limited by the bottleneck buffers within the network. We

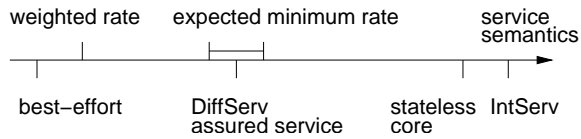


Fig. 1. Network QoS spectrum. It illustrates a range of QoS from best-effort service, differentiated service to rate and delay guaranteed service. Weighted rate service and expected minimum rate service locate between the best-effort service and the differentiated service.

overcome this constraint by leveraging an Active Queue Management (AQM) mechanism that communicates the virtual queueing delay [7] [31] incurred on a virtual queue [19]. With such an AQM mechanism, we achieve near-zero queue and high utilization at the congested routers.

Figure 1 illustrates a *qualitative* spectrum of packet-switching network QoS capabilities ranging from best-effort service, DiffServ, to rate/delay guaranteed service offered by IntServ, including frameworks such as Stateless Core (SCORE) [29]. Services on the right-hand side of the diagram are more complex and offered at finer granularity. The left side of the spectrum implies less quantitative services, the use of FIFO queuing, closed-loop congestion control and potentially AQM mechanisms inside the network. Our framework resides in the middle of the spectrum, to the left of DiffServ assured service in the sense that we do not impose the complexity required to implement drop precedence inside the network, but to the right of DiffServ in the sense of the wide service range achieved. Unlike IntServ and SCORE that offer per-packet assurances, our service semantics are meaningful only in steady state due to the use of the closed-loop congest control. In other words, our model offers the lower end of the service spectrum at very low complexity.

We evaluate the EMR and WRS building blocks using ns-2 [26] simulations and Linux implementation experiments. Several fundamental issues such as graceful service degradation (when there is oversubscription, limits on accumulation, or underprovisioned bottleneck buffer size) and trade-offs (like non-AQM droptail vs. optional AQM support at bottlenecks) are explored. We note that this paper only develops the abstract service model, albeit with ns-2 simulation and Linux implementation validation, and does not explore architectural issues such as multi-ISP service coordination, etc.

This paper is organized as follows. In Section II we review the related work. In Section III we describe the ACC fluid model and Monaco, one of the ACC schemes, that serves as the basis on which we design the EMR service building block in Section IV and the

WRS service building block in Section V. A set of ns-2 simulation results are given in Sections IV-C and V-B. In Section VI we multiplex all the services to show that they can co-exist in a complex network. Section VII discusses possible applications of our scheme and some open issues. Section VIII concludes this paper.

## II. RELATED RESEARCH

IntServ architecture [5] was proposed to provide end-to-end bandwidth and delay guarantees. But there is no real deployment seen due to its algorithm complexity and that it has to maintain per-flow state inside the routers. By carrying the per-flow state in the packet headers and thus eliminating them from inside the routers, SCORE [29] is a significant step toward achieving guaranteed service while keeping the core Internet stateless.

DiffServ [4] was developed to implement scalable service differentiation in the Internet. It defines an assured forwarding service that provides delivery of IP packets in four independently forwarded classes with three different levels of drop precedence. Wang proposed a differentiated service scheme called “User-Share Differentiation” that allows ISPs to differentiate traffic flows on a per-user basis, providing minimum bandwidth guarantees and share-based bandwidth sharing [30].

Clark and Fang suggested that each flow uses a “profile” specifying how much capacity should be allocated to TCP connections during congestion [8]. A component is placed at the edge of the network that marks a bit in the passing packet headers to denote whether the packets are in- or out-of-profile. The bottleneck then uses two RED algorithms [11] in parallel to drop the packets randomly during congestion with preference toward keeping the packets that are marked in-profile.

All the proposals discussed above are basically open-loop approaches. Researchers have also designed closed-loop mechanisms to provide service differentiation. For instance, Crowcroft et al. implemented MultTCP which makes a connection behave as  $w$  TCP connections by increasing the congestion window of the single MultTCP connection by  $w$  packets in each RTT and, when a loss occurs, decreasing it to only  $\frac{w-0.5}{w}$  [9]. Nandagopal et al. provided a systematic analysis on how to adjust TCP Reno’s increase/decrease parameters to achieve the weighted bandwidth differentiation [25]. In both works the service is achieved by (adaptively) changing the increase/decrease parameters of the congestion control. Hsieh et al. tried to combine parallel TCP connections [14]. In this paper we take a different approach to achieve service differentiation by manipulating accumulation allocation among the competing flows.

A different line of research started from Kelly’s optimization framework [16], followed by Low et al. [21], Srikant et al. [18], and Massoulié et al. [23], where they model network congestion control as a nonlinear optimization problem under which all the users try to maximize their own interest, subject to a set of capacity constraints. Our ACC scheme fits into this optimization framework. Kunniyur and Srikant developed an Adaptive Virtual Queue (AVQ) algorithm [19] which we leverage to keep a small physical queue in the congested routers (see Section IV-A). Low et al. proposed an optimization model [22] for TCP Vegas [6] and suggested to improve its performance by using a buffer management mechanism called Randomly Exponential Marking (REM) [1]. All these works were developed for the purpose of congestion control. In this paper, we extend ACC as a data-plane building block to provide service differentiation and guarantees.

### III. BACKGROUND

In this section we briefly describe our prior work on the ACC fluid model and its packet-switching network implementation, the Monaco scheme. Monaco solves the technical problems of Vegas and thus serves as a basis for the work in this paper. For the complete description of ACC and Monaco, the reader is referred to [31].

#### A. ACC Fluid Model

We define the accumulation concept using a bit-by-bit fluid model. Then we develop a congestion control algorithm based on accumulation and show its steady state properties.

1) *Accumulation*: Consider an ordered sequence of FIFO nodes  $\{R_1, \dots, R_J\}$  along the path of a unidirectional flow  $i$ . The flow comes into the network at the ingress node  $R_1$  and, after passing some intermediate nodes  $R_2, \dots, R_{J-1}$ , goes out from the egress node  $R_J$ .<sup>1</sup> The propagation delay from node  $R_j$  to node  $R_{j+1}$  is a constant  $d_j$ .

Define flow  $i$ ’s accumulation as a time-shifted, distributed sum of the queued bits in all the nodes along its path from  $R_1$  to  $R_J$ :

$$a_i(t) = \sum_{j=1}^J q_{ij}(t - \sum_{k=j}^{J-1} d_k) \quad (1)$$

where  $q_{ij}(t - \sum_{k=j}^{J-1} d_k)$  is flow  $i$ ’s bits queued in node  $R_j$  at time  $t - \sum_{k=j}^{J-1} d_k$ . Note it includes only those bits

<sup>1</sup>We can map  $R_1/R_J$  nodes as source/destination end hosts to form an end-to-end control loop or ingress/egress edge routers to form an edge-to-edge control loop. We discuss practical issues in Section VII.

backlogged inside the node buffers, not those stored on transmission links. This definition serves as a reference to implement an unbiased accumulation estimator in Section III-B. We aim to control the flow rate by controlling its accumulation.

2) *Control Algorithm*: We apply a window-based control to use accumulation as a measure to detect network congestion. If accumulation is low, we increase the congestion window; otherwise, we decrease it to drain accumulation. Specifically, we try to maintain a constant target accumulation  $a_i$  for each flow  $i$  using a proportional ACC control algorithm:

$$\dot{w}_i(t) = -\frac{\kappa}{rtt_i} \cdot (a_i(t) - a_i) \quad (2)$$

where  $\kappa > 0$ ,  $w_i(t)$ ,  $rtt_i$ ,  $a_i(t)$  and  $a_i$  are respectively the congestion window size, round trip time, instantaneous accumulation and target accumulation value of flow  $i$ .

3) *Properties*: Congestion control can be formalized as a resource allocation problem [16] [21] [18] [24]. Using steady state queuing analysis and nonlinear optimization we showed in [31] that the above ACC control algorithm fits into the Kelly framework [16] and drives the network to an equilibrium of weighted proportional fairness, with target accumulation  $a_i$  as flow  $i$ ’s weight. *It is this weight  $a_i$  that enables service differentiation*. In principle, since the equilibrium is decided by all  $a_i$ ’s, we can accordingly adjust  $a_i$  to steer the equilibrium in order to achieve a specific service, e.g., EMR or WRS rate allocations discussed in Sections IV and V. This allows us to avoid the major pitfalls in the loss-based service differentiation approaches, as discussed in Section V-C.

#### B. Monaco Scheme

Based on the measurement and control of accumulation, we have shown that a family of congestion control schemes can be derived [31]. One example is TCP Vegas which estimates accumulation as  $sending\_rate \times (rtt - rtt_p)$  at the sender side, where  $rtt$  is round trip time (RTT) and  $rtt_p$  refers to round trip propagation delay. The Vegas accumulation estimator is sensitive to both the measurement error of the propagation delay and reverse path congestion. Therefore we designed a receiver-based, out-of-band Monaco scheme that ensures robust accumulation estimation.

1) *Accumulation Estimation*: Monaco estimates accumulation at the *receiver* side. It generates a pair of back-to-back control packets once per RTT at the sender as shown in Figure 2. One control packet is sent out-of-band (OB) and the other in-band (IB). The OB control packet skips queues in the intermediate routers by passing through a separate dedicated high priority queue.

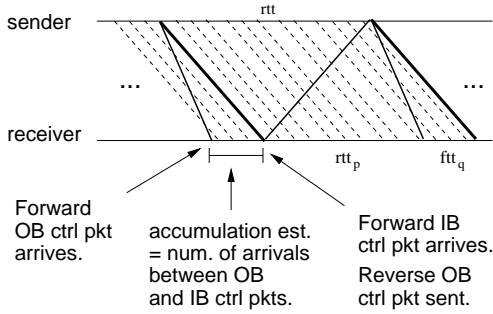


Fig. 2. Monaco accumulation estimator generates a pair of back-to-back OB and IB control packets once per RTT at the sender. The number of data packets at the receiver between the OB and IB control packets is measured as accumulation, which is sent back to the sender using a reverse OB control packet.

Assuming the OB queues to be minimal as only other OB control packets share them, such packets experience only the propagation delay in the forward path. The IB control packet goes along with the regular data packets and reaches the receiver after experiencing the current queuing delay in the network. The time interval between the OB and IB control packets measured at the receiver samples the sum of the queuing delays in the forward path. Considering a network in steady-state with enough buffers where there is no packet loss, then, by Little's law, the average number  $\hat{a}_M$  of data packet arrivals at the receiver after the OB control packet, but before the IB control packet equals the average accumulation.

Obviously this comes with an extra requirement of two separate FIFO queues inside the network routers, with a high priority queue for the OB control packets and a low priority queue for the IB control packets and the data packets.<sup>2</sup>

2) *Control Policy*: Monaco employs the proportional control policy in Equation (2). It tries to maintain a constant target accumulation  $a_i$  for each flow  $i$  by adjusting its congestion window according to:

$$cwnd_i(n+1) = cwnd_i(n) - \kappa \cdot (\hat{a}_{iM} - a_i) \quad (3)$$

where  $\hat{a}_{iM}$  is the accumulation estimate,  $\kappa$  is set to 0.5, and  $cwnd_i(n)$  is the congestion window value at a control period  $n$ . In addition we conservatively bound the increase to within one MTU per RTT.

Monaco sender implements rate-based pacing to smooth incoming traffic into the network using a token

<sup>2</sup>As designed, Monaco can be used to control flow aggregates or individual TCP/UDP connections. When integrated with TCP, the IB and OB control packets can bear TCP segments. The IB control packet is the packet bearing the TCP segment with the next sequence number after the OB packet's TCP segment. The accumulation estimate can be fed back as a TCP option header. Thus ACC-based service differentiation can be implemented without adding new packets to the network.

bucket shaper with a rate value of  $cwnd/rtt$  to alleviate traffic burstiness. It also includes reliability enhancements for the control and data packets lost. The reader is referred to [31] for more details.

#### IV. EXPECTED MINIMUM RATE SERVICE

In this section we demonstrate the EMR service building block. We aim to provide any flow *a contracted (or expected minimum) bandwidth plus a proportional share of remaining capacity*. It is achieved by keeping an appropriate amount of accumulation inside the network for that flow. We mean "expected" in the sense that the minimum can be satisfied if there is no oversubscription. If there is, obviously we can not fulfill all the demands. Therefore a graceful service degradation is defined. We show the theoretic results for a general network topology and evaluate them using a set of ns-2 simulations based on Monaco.

##### A. Algorithm

Let's consider a network of a set  $L = \{1, \dots, |L|\}$  of links, shared by a set  $I = \{1, \dots, |I|\}$  of flows. Each link  $l \in L$  has capacity  $c_l$ . Flow  $i \in I$  passes a route  $L_i$  consisting of a subset of links, i.e.,  $L_i = \{l \in L \mid i \text{ traverses } l\}$ . A link  $l$  is shared by a subset  $I_l$  of flows where  $I_l = \{i \in I \mid i \text{ traverses } l\}$ .

As we discuss in Section III-A.3, a specific rate allocation corresponds to a particular equilibrium of the control algorithm (2); and, in turn, the equilibrium is decided by the target accumulation  $a_i$ . So service provisioning is mapped to the allocation of the target accumulations. We use the following steady state analysis to introduce our algorithm.

Suppose we provide flow  $i$  a bandwidth  $x_i^*$  that is the sum of an EMR  $x_{ie}$  and a proportional share  $x_{ip}^*$  of the remaining network capacity<sup>3</sup>:

$$x_i^* = x_{ie} + x_{ip}^*. \quad (4)$$

We achieve this allocation by keeping for flow  $i$  a total accumulation  $a_i$  that, correspondingly, also includes two parts:  $a_{ie}$  for  $x_{ie}$  and  $a_{ip}$  for  $x_{ip}^*$ , i.e.,

$$a_i = a_{ie} + a_{ip}. \quad (5)$$

According to Little's law, we have

$$a_i = x_i^* \cdot t_{iq}, \quad (6)$$

$$a_{ie} = x_{ie} \cdot t_{iq}, \quad (7)$$

$$a_{ip} = x_{ip}^* \cdot t_{iq} \quad (8)$$

<sup>3</sup>The reason we use the symbols  $x_i^*$  and  $x_{ip}^*$  instead of  $x_i$  and  $x_{ip}$  here and we call  $x_{ip}^*$  a proportional share is that  $x_i^*$  and  $x_{ip}^*$  are solutions to a nonlinear optimization, while  $x_{ie}$  is an input parameter.

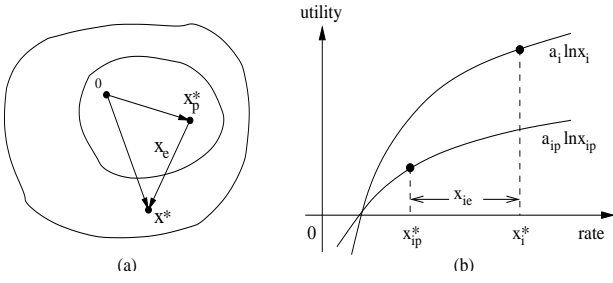


Fig. 3. EMR could be modeled as two simultaneous nonlinear optimization problems: (a) Convex constraint sets showing  $x^* = x_e^* + x_{ip}^*$ : the inner one for  $x_{ip}$  while the outer one for  $x_i$ ; (b) Logarithmic utility functions of  $x_i$  and  $x_{ip}$ .

where  $t_{iq}$  is the steady state queueing delay experienced by flow  $i$  in its forward path. Equations (5)-(8) lead to

$$a_{ip} = \left(1 - \frac{x_{ie}}{x_i^*}\right) \cdot a_i \quad (9)$$

where  $x_{ie}$  is the expected rate known *a priori*,  $x_i^*$  can be measured at either the sender or the receiver, and  $a_i$  is provided by the accumulation estimator.

Obviously, if we keep constant accumulation for a flow, then its (proportionally fairly) allocated rate is decided by network routing and other competing flows. If we want to keep a constant rate for a flow, independent of the changing environment, then the corresponding accumulation has to adapt. This is reflected by  $t_{iq}$  in Equation (7), the queueing delay which is changing in a dynamic environment. To avoid setting a varying parameter  $a_{ie}$ , or equivalently  $a_i$  in Equation (6), we use Equation (9) to calculate  $a_{ip}$  that represents the accumulation in excess of the accumulation imposed by the expected minimum rate  $x_{ie}$ . We steer the system so that  $a_{ip}$  approaches a target accumulation, a preset value (three packets in this paper) that is the same for all the flows. This can be modeled by the following two nonlinear optimization problems.

Firstly let's assume enough buffers are provided in all the congested routers and there is no oversubscription. We consider the total rate  $x_i^*$  achieved with corresponding accumulation  $a_i$ . As proved in [31], the flow rate  $x_i^*$  is the unique maximum of the following nonlinear optimization problem related to  $a_i$ :

$$\text{maximize} \quad \sum_{i \in I} a_i \ln x_i \quad (10)$$

$$\text{subject to} \quad \sum_{i \in I_l} x_i \leq c_l, \quad \forall l \in L \quad (11)$$

$$x_i > 0, \quad \forall i \in I$$

meaning that  $x_i^*$  achieves weighted proportional fairness:

$$\sum_{i \in I} a_i \cdot \frac{x_i - x_i^*}{x_i^*} \leq 0 \quad (12)$$

where  $x_i$  is any feasible rate allocations satisfying the constraint (11).

Beyond the expected rate  $x_{ie}$ , we then consider the rate  $x_{ip}^*$  achieved with corresponding accumulation  $a_{ip}$ . Similarly we can prove that the flow rate  $x_{ip}^*$  is the unique maximum of the residual problem related to  $a_{ip}$ :

$$\text{maximize} \quad \sum_{i \in I} a_{ip} \ln x_{ip} \quad (13)$$

$$\text{subject to} \quad \sum_{i \in I_l} x_{ip} \leq c_l - \sum_{i \in I_l} x_{ie}, \quad \forall l \in L \quad (14)$$

$$x_{ip} > 0, \quad \forall i \in I$$

meaning  $x_{ip}^*$  achieves similar proportional fairness:

$$\sum_{i \in I} a_{ip} \cdot \frac{x_{ip} - x_{ip}^*}{x_{ip}^*} \leq 0 \quad (15)$$

where  $x_{ip}$  is any feasible rate allocations satisfying the constraint (14).

So a system providing an EMR service actually does two nonlinear optimization problems. However, these two problems are not independent – they are *simultaneous* in that as long as one problem achieves its optimality, the other also achieves its optimality at the same time. We illustrate this result in Figure 3. The reader is referred to Section 5.3 of [13] for an analysis regarding general utility functions.

If the assumptions do not hold, i.e., there is either oversubscription or underprovisioned buffers, then the above two optimalities are often not realized in a real network. There are three boundary conditions affecting the realizability of EMR:

- Oversubscription: Without admission control, the constraint (14) might be always invalid. Or it is possible that

$$\sum_{i \in I_l} x_{ie} \geq c_l, \quad \exists l \in L; \quad (16)$$

- Accumulation limit: To avoid intolerably long queues, we introduce an upper bound  $A_i$  on accumulation, namely,

$$a_i = \sum_{l \in L_i} q_{il} \leq A_i, \quad \forall i \in I; \quad (17)$$

- Buffer overflow: Even with the above accumulation limit, we can not guarantee that each router buffer  $Q_l$  is sufficiently provisioned, i.e.,

$$q_l = \sum_{i \in I_l} q_{il} \leq Q_l, \quad \forall l \in L. \quad (18)$$

When any of the boundary conditions is effective, EMR can not be satisfied. Therefore we need to define a degraded service for this case.

Firstly, we argue that the constraints (16) and (18) can be translated equivalently into the form of (17). For (18), it is obvious because both (17) and (18) are constraints on  $q_{il}$ . For (16), the intuition is that when there is an oversubscribing flow, its expected minimum rate cannot be satisfied even were it to incur infinite accumulation, which means before this happens, its accumulation constraint (17) will be effective. So these three constraints can be summarized into one form of (17) with an equivalent accumulation limit  $A_i^{eq}$ . To take into account all the above boundary conditions (16)~(18), we define a new optimization problem similar to (10) but with changed coefficients  $a'_i$  and thus different, though still logarithmic, utility functions:

$$\begin{aligned} & \text{maximize} && \sum_{i \in I} a'_i \ln x'_i && (19) \\ & \text{subject to} && \sum_{i \in I_l} x'_i \leq c_l, \forall l \in L \\ & && x'_i > 0, \forall i \in I \end{aligned}$$

where

$$a'_i = \min(a_i, A_i^{eq}), \forall i \in I. \quad (20)$$

Again, its optimal allocation  $x'_i^*$  achieves weighted proportional fairness:

$$\sum_{i \in I} a'_i \cdot \frac{x'_i - x'_i^*}{x'_i^*} \leq 0 \quad (21)$$

where  $x'_i$  is any feasible rate allocations.

Consequently, when there is either oversubscription, accumulation limit, or underprovisioned buffers, these conditions affect the realization of (10) and (13), i.e., EMR can not be provisioned. A new optimization problem (19) is automatically defined by adding these constraints (16)~(18) into (10), achieving a weighted proportional rate allocation which can be computed from the boundary conditions. The weight is changed from  $a_i$  to  $a'_i$  defined by Equation (20). As a result, EMR gracefully degrades into a weighted proportionally fair rate, with a new set of weights  $a'_i$ 's. Further, since we have the freedom to set the accumulation limit  $A_i$  for each flow  $i$  in (17), this parameter provides a policy-based control on bandwidth allocation. We discuss how to set  $A_i$  in Section IV-B and use simulations to illustrate  $A_i$ 's effect in Section IV-C.

Now let's look at a trade-off. Even if we set an accumulation limit for each flow, the steady state queuing delay or physical queue length might be too large as the number of flows increases. Is it possible to provide the requested services based on managing accumulation and, at the same time, keep a small steady state queue? We have adopted the AVQ algorithm [19] that emulates an

adaptively changing link capacity such that the steady state queue is sufficiently small. We compute a virtual queueing delay [7] defined as the ratio of virtual queue length divided by virtual capacity and add it into the forward control packet provided by the out-of-band accumulation estimator<sup>4</sup>. We call this mechanism Adaptive Virtual Delay (AVD) algorithm. A nice property of AVD is that it is incrementally deployable since a mixed set of non-AQM droptail and AVD routers can work together (see Section VI and [31]). In such an environment the accumulation estimate will be  $\hat{a} = \hat{a}_{FIFO} + x \cdot \hat{t}_{VD}$  where  $\hat{a}_{FIFO}$  is the accumulation in those FIFO routers,  $x$  is the received rate and  $\hat{t}_{VD}$  is the sum of all the virtual delays at those AVD routers.

To sum up, we use the algorithm below to provide the EMR service. It includes seven steps.

---

**Algorithm 1** Expected Service Pseudo-code at Sender

---

*cwnd* = the congestion window in bytes  
*pwnd* = the congestion window in the previous RTT  
*ssthresh* = the slow start threshold  
*srtt* = the smoothed RTT estimation  
*A* = the total accumulation limit  
*a<sub>p</sub>* = the target accumulation beyond the EMR  
*a(t)*, *a<sub>p</sub>(t)* = accumulation estimates

- (1)  $x(t) = pwnd * 8.0 / srtt$ ;
- (2)  $a_p(t) = \max(a(t) * (1 - x_e/x(t)), 0.0)$ ;
- (3)  $pwnd = \min(pwnd + mtu, cwnd)$ ;
- (4)  $cwnd = pwnd - k * \max(a_p(t) - a_p, a(t) - A)$ ;
- (5) if  $(a(t) > A \parallel a_p(t) > a_p)$   $ssthresh = cwnd$ ;
- (6) else {
  - (6.1) if  $(pwnd + mtu \geq ssthresh)$   
 $ssthresh = cwnd$ ;
  - (6.2)  $cwnd = \min(pwnd * 2.0, ssthresh)$ ;
- (7)  $rate\_limit = cwnd * 8.0 / srtt$ ;

---

In Step 1, we compute the departure rate  $x$  as the bits transmitted in the last RTT divided by the smoothed RTT, or  $srtt$ .

In Step 2, we compute the accumulation  $a_p$  incurred beyond the EMR according to Equation (9). When a control loop is ramping up or during oversubscription, the departure rate  $x$  may be less than the EMR  $x_e$ , causing  $a_p$  to be negative. So we max with 0.0 to force nonnegativity.

In Step 3, we force a  $pwnd$  that is within 1 MTU of

<sup>4</sup>This accumulation estimator (see Section III-A.1) sends a control packet once per RTT out-of-band to avoid standing queues that affect the Vegas accumulation estimator. If no control packet is available from the accumulation estimator then the virtual delay may be communicated using bit marking as in REM [1].

$cwnd$  to be equal to  $pwnd$ . This is necessary because our algorithm stops sending when the packet at the head of the queue would cause  $pwnd$  to exceed  $cwnd$ .

In Step 4 we set the congestion window according to the Monaco control policy defined in Equation (3) and the accumulation limit  $A$ .

In Steps 5–6, we determine whether step 4 was a decrease or an increase step. In Step 5, we stop a slow start by reducing  $ssthresh$  to the current congestion window size. In other words, each control loop slow-starts until congestion is first detected. Step 6.1 ensures that when a  $cwnd$  decreases due to something other than congestion (e.g., decreasing user demand),  $ssthresh$  does not decrease, i.e.,  $ssthresh$  tracks the congestion level in the network rather than the user demand. It bounds the increase step to one MTU per RTT. Thus Monaco increases no more aggressively than TCP’s additive-increase-multiplicative-decrease (AIMD) and less aggressively than TCP in the neighborhood of the equilibrium. Though not shown here, Monaco backs off by one half in response to loss and thus Monaco degrades to TCP in the presence of significant loss. Step 6.2 bounds slow start by  $ssthresh$ .

Step 7 sets the rate on the token bucket shaper used in Monaco’s rate-based pacing.

### B. How to Set the Accumulation Limit

One question remaining is how to set the accumulation limit  $A_i$ , which serves as a policy-controlled parameter for an EMR flow  $i$ . Obviously, a flow with a larger  $A_i$  has more chance to get its EMR during oversubscription; a smaller  $A_i$  means its EMR will probably not be obtained in the same situation.

By the definition in Equation (1), the accumulation of a flow is distributed in the form of the buffered packets among the congested routers on its path. According to Equation (5), to achieve EMR, accumulation  $a_i$  includes two parts:  $a_{ip}$  steers toward three packets, the default value we set for a general non-EMR flow;  $a_{ie}$  should adapt according to the changing environment. Since  $A_i$  is an upper bound of  $a_i$ , it should be set in proportion to the number of the congested routers and how congested they are. This makes setting  $A_i$  an open question in theory when there is no AVD deployed inside the network routers. In this case  $A_i$  is limited by the buffer available in the congested routers in the network, but this is difficult to know from the network edges. In practice this assumes a management plane that can collectively set  $A_i$ . This management plane monitors the network for significant packet loss due to buffer overflow and scales  $A_i$  appropriately to minimize the loss. Once the

loss has been minimized,  $A_i$  can be set relative to each other based on policy as described below for a network of AVD routers.

In scenarios where AVD is used,  $A_i$  no longer refers to physical queuing and thus we are free to use  $A_i$  as purely a policy-based mechanism<sup>5</sup> for defining how bandwidth is distributed during oversubscription. If all  $A_i$  are set equal then expected minima tend to be satisfied in “smallest first” order. If all  $A_i$ ’s are set in proportion to their expected minima, then “all-or-none” of the expected minima are satisfied. We can also define gold and silver services wherein all the gold members share one accumulation limit which is larger than the accumulation limit shared by all the silver members. When possible, gold members are satisfied first; otherwise, the ratio between the gold and silver accumulation limits refers to the ratio of their proportional shares if oversubscription arises.

We illustrate this issue using concrete simulation examples in the next subsection and Section VI.

### C. Simulations

We evaluate the performance of the EMR service building block using ns-2 simulations on a single bottleneck. Each flow has a different propagation delay. In Section VI we provide ns-2 simulation and Linux implementation results for a more complex network of multiple bottlenecks. In all the experiments we set data packet size to 1KB.

We simulate a single 100Mbps bottleneck shared by ten flows using Monaco. We use simulation because this allows us to temporarily set aside the practical limitation of finite buffer sizes, so that we can study the range of services in the absence of packet loss caused by underprovisioned buffer. Flow 0 has an EMR  $x_{0e}$  while other nine flows request a proportional rate service (i.e., with an EMR of 0). Each source  $i$  ( $0 \leq i \leq 9$ ) is connected to the bottleneck via an 1Gbps link with one-way propagation delay  $11i + 1$ ms. We perform two kinds of simulations, one using a non-AQM droptail bottleneck, the other using an AVD bottleneck.

In the first set of simulations we evaluate the range of satisfiable EMRs without AQM and we demonstrate the effects of setting the accumulation limit. For each accumulation limit of 30KB and 3000KB, we run simulations each with a different expected rate  $x_{0e}$  from 0 to

<sup>5</sup>Setting  $A_i$  and the expected minima both assume coordination at the service provider level. In end-to-end scenarios, this is only tractable if we assume DiffServ-like building blocks for policing at provider edges along with a management infrastructure for brokering capacity.

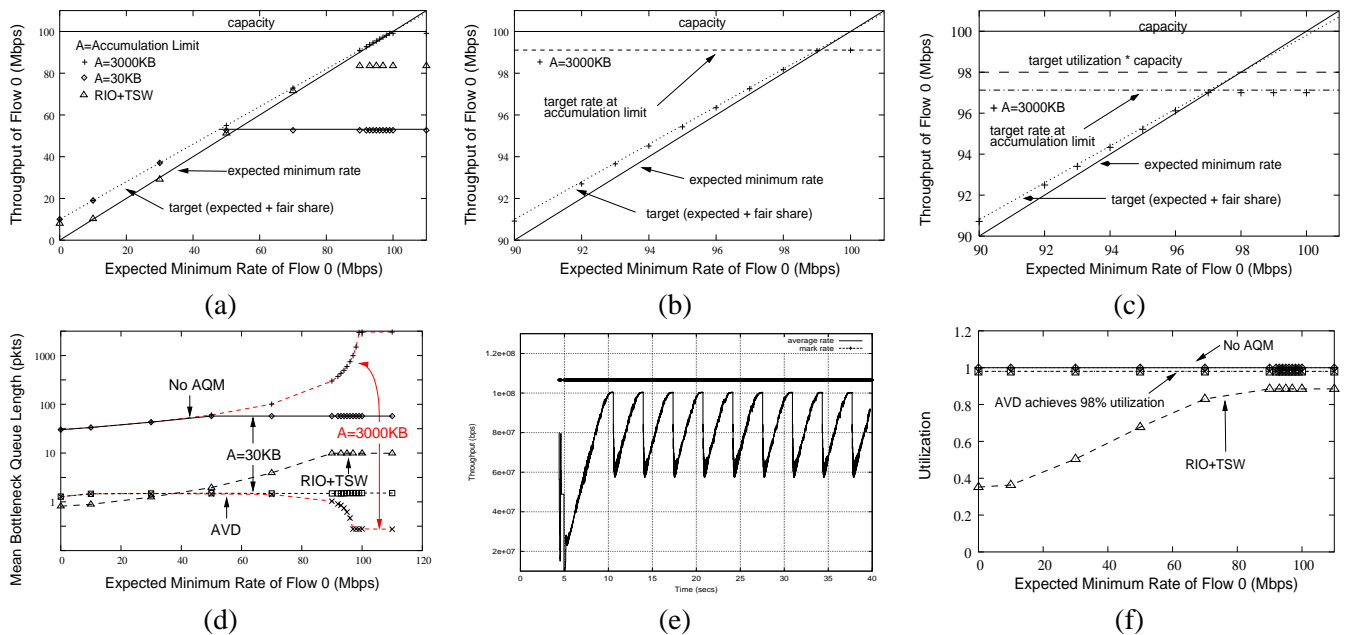


Fig. 4. EMR in a single bottleneck: (a) Monaco throughput  $x_0$  vs. EMR  $x_{0e}$  with a non-AQM droptail bottleneck and RIO throughput vs. DiffServ bandwidth allocation; (b) The former graph zoomed into 90-101Mbps; (c) Monaco throughput  $x_0$  vs. EMR  $x_{0e}$  with an AVD bottleneck, zoomed into 90-101Mbps; (d) Steady state queue length vs. EMR  $x_{0e}$  with a droptail or AVD bottleneck (when flow 0's accumulation limit  $A$  is set to 30KB and 3000KB, respectively), and RIO+TSW average queue length vs. DiffServ bandwidth allocation; (e) RIO+TSW's measured rate for capacity allocation 80Mbps; (f) Bottleneck utilization when using Monaco and RIO+TSW. In these simulations, we set  $\kappa=0.5$ , target accumulation  $a_p=3\text{KB}$ , AVD's damping factor  $\alpha=0.1$  and target utilization  $\beta=0.98$ . For RIO+TSW simulations we use the parameters in [8].

110Mbps. All other flows have a target accumulation of 3KB. The result is shown in Figure 4(a) and zoomed in Figure 4(b). With  $A = 3000\text{KB}$ , we are able to allocate up to 99.1Mbps (i.e.,  $\frac{3000 \times 100}{3000 + 9 \times 3}$ ) of the 100M bottleneck to a single flow before the accumulation limit is reached. When  $A = 30\text{KB}$ , the maximum satisfiable EMR is  $\frac{30 \times 100}{30 + 9 \times 3} = 52.6\text{Mbps}$ , demonstrating that the unsatisfied EMR due to the constraint (17) degrades EMR to a weighted proportionally fair rate.

The upper part of Figure 4(d) shows that the queue length grows dramatically (note the logarithmic scale of the vertical axis) as the EMR  $x_{0e}$  increases. This is most apparently shown by the case when  $A = 3000\text{KB}$ . However in all cases, the queue growth flattens when the accumulation limit is reached. The rapid queue growth as the EMR approaches the available capacity demonstrates the bound on the achievable services as a function of the bottleneck buffer size in the network.

In the second set of simulations, we repeat the same scenario except with an AVD bottleneck. The range of achieved EMRs is similar to the case without AQM, as shown in Figure 4(c) for the EMR of 90-100Mbps. However, AVD keeps the queue length at near zero as depicted in the lower part of Figure 4(d), since instead of incurring physical accumulation, each control loop incurs virtual accumulation on a virtual queue. In fact

the average queue diminishes as the ratio of the rates increases since 1) the packets in the fast flow are nearly evenly spaced due to rate-based pacing and therefore do not incur queue, and 2) the slower flows send so infrequently that they rarely perturb the queue.

As shown in Figure 4(f), the bottleneck utilization for all cases without AQM was 100% in the steady state (since the queue never drains completely), and when AVD was used, the utilization was always within half a percent of 98%, our target utilization for AVD.

Now we compare EMR and DiffServ assured service using a set of simulations. We replace all Monaco flows with TCP Reno connections. We vary the allocation for one TCP Reno connection using Clark et al.'s RIO building blocks [8]. To perform marking they propose the Time Sliding Window (TSW) tagger which marks packets in-profile so long as the connection sends with rate less than  $4/3$  of its allocation specified in its profile. Because TCP backs off one half of its congestion window in response to loss, the expectation is that during congestion the TCP connection should sawtooth between  $2/3$  and  $4/3$  of its allocation, resulting in a long-term average rate near the allocation. RIO uses two RED [11] algorithms in parallel to randomly drops "in" and "out" packets in the queue. The RED algorithms are configured such that the "out" packets are dropped before the "in"



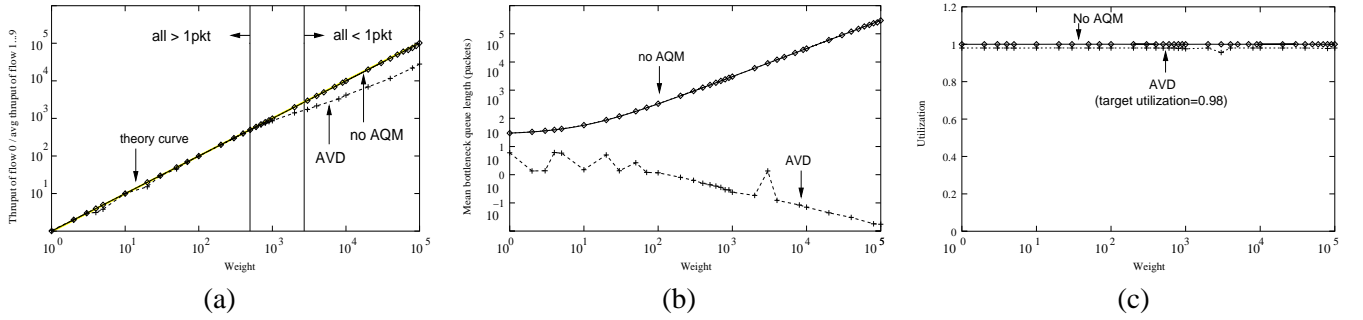


Fig. 5. WRS in a single bottleneck: (a) Relative throughput ratio vs. weight; (b) Bottleneck queue vs. weight; (c) Bottleneck utilization. In these simulations, we set  $\kappa=0.5$ , target accumulation  $a_i=w_i*3\text{KB}$ , AVD's damping factor  $\alpha=0.1$  and target utilization  $\beta=0.98$ .

packets. We use the same parameter settings for RIO and TSW as specified in Table 1 of [8]. Additionally our RIO algorithm has Explicit Congestion Notification (ECN) [28] turned on. Thus packets are marked for congestion (different than the in/out mark) when RIO would otherwise have dropped.

In Figure 4(e) we demonstrate one of the limitations of the TSW tagger and a more fundamental limitation of providing assured services with TCP+RIO. First a connection receives the same treatment for any allocation greater than 3/4 of the bottleneck capacity since all the packets are marked in-profile. More importantly, in order to obtain an allocation that is a significant fraction of the bottleneck capacity, TCP must oscillate its window size on the same order as the bottleneck capacity. This oscillation is a consequence of TCP's AIMD algorithm and thus affects all profile marking, ECN marking, and AQM algorithms. Since the amplitude of this sawtooth grows roughly linearly with flow rate, accommodating a flow with a large bandwidth allocation implies one of the following three: large queues (see Figure 4(d)), limits on achievable allocations (as shown for bandwidth allocations above 80Mbps in Figure 4(e)), or low utilization (as shown in Figure 4(f) for bit rates below 80Mbps). This *fundamental* limitation of TCP+RIO makes it impossible to simultaneously achieve high utilization, low queue length, and a wide disparity in the allocated rates. By avoiding AIMD, Monaco with AVD simultaneously achieves all three.

## V. WEIGHTED RATE SERVICE

In this section we propose the WRS service building block. Our goal is to provide *weighted rate discrimination among flows along the same path, i.e., a flow with weight  $w$  should get a bandwidth  $w$  times that of a flow with weight 1*. We show the steady state queuing theoretic result for a general network topology. Then we evaluate it using ns-2 simulations and show that the

achieved WRS range significantly outperforms the loss-based approaches by *three orders of magnitude*.

### A. Algorithm

Again let's consider the general network topology described in Section IV-A from a steady state queuing analysis perspective. At a steady state in any bottleneck link  $l$  where

$$\sum_{i \in I_l} x_i = c_l \quad (22)$$

we have its steady state queue length  $q_l$  including contributions from a subset of flows traversing that link as

$$q_l = \sum_{i \in I_l} q_{il} \quad (23)$$

where  $q_{il}$  is flow  $i$ 's steady state queue at bottleneck  $l$ .

We use window-based congestion control, in which a window  $w_i$  bits of flow  $i$  could be stored either on transmission links ( $= w_i - a_i$ ) or in router buffers as steady state accumulation

$$a_i = \sum_{l \in L_i} q_{il} \quad (24)$$

where  $L_i$  is the subset of bottleneck(s) which flow  $i$  traverses. If two flows  $i_1$  and  $i_2$  traverse the same path from a source to a destination, then they share the same set of bottleneck(s), namely,

$$L_1 = L_2. \quad (25)$$

At any shared bottleneck  $l$  employing FIFO scheduler which decides packet departure totally based on its arrival order, the flow rate allocation is proportional to the buffer allocation (if loss amount is neglectable), i.e.,

$$\frac{x_1}{x_2} = \frac{q_{1l}}{q_{2l}}. \quad (26)$$

The above three equations lead to

$$\frac{x_1}{x_2} = \frac{\sum_{l \in L_1} q_{1l}}{\sum_{l \in L_2} q_{2l}} = \frac{a_1}{a_2} \quad (27)$$

which means that, for a general network topology, the rate allocation to flows along the same path is proportional to the accumulation allocation. Further, it is the *relative* accumulation allocation, instead of the *absolute* accumulation allocation, that decides the rate differentiation.

## B. Simulations

We evaluate the performance of the WRS service building block using ns-2 simulations on a single bottleneck with large enough buffer size to avoid packet loss. For a more realistic network of multiple congested links shared by flows passing through different numbers of bottlenecks, we provide ns-2 simulation and Linux implementation results in Section VI.

We use the same single bottleneck network where an 100Mbps link is shared by ten flows with very heterogeneous RTTs. Flow 0 has a varying weight  $w$  while other flows have unit weight (i.e,  $a_0 = wa_1 = \dots = wa_9$ ). We performed two sets of simulations to evaluate the weighted service differentiation range.

In the first set of simulations we evaluate the service differentiation range without AQM. We did a set of simulation runs by changing  $w$  from 1 to  $10^5$  which is at least three orders of magnitude larger than the weights (10~100) achieved with TCP in [9] [25]. We discuss this huge difference in the next subsection. As shown by the upper curve in Figure 5(a), for the wide range of weight variation, accurate weighted sharing is achieved. This comes with a cost, though. The upper curve in Figure 5(b) shows that the steady state queue length at the bottleneck increases linearly with weight. The curvature in the mean queue length in Figure 5(b) is due to a y-offset for a weight 1 equal to the sum of the target accumulations (30KB). As with the EMR building block, the large queue incurred by service differentiation based on physical accumulation demonstrates the practical bound on service differentiation that could be achieved with finite bottleneck buffer sizes.

Again, with AVD we are able to break the coupling between the notion of accumulation and real queuing. This is shown by our second set of simulations. Figure 5(b) demonstrates that AVD achieves average queue sizes less than 1 packet. This average diminishes as weight increases for the same reason that average queue diminishes as EMR increases as we already discussed in Section IV-C: control loops that send rarely also rarely perturb the queue.

As shown in Figure 5(a), for weights below  $10^3$ , AQM achieves the desired weighted share. However, above about  $10^3$ , the control loop with the large weight obtains

less than the desired weighted share. This arises because AVD holds the loops with weight 1 at a window size of one. In this regime, the Monaco control policy is no longer defined, instead if the accumulation estimate is larger than the target and the window size is one then the control loop halves its shaper's send rate. Once the accumulation estimate reduces below the target, we reset the respective shaper to a rate of 1 packet per RTT. From simulation to simulation, as we increase the weight of source  $S_0$  to 491, the equilibrium window size of source  $S_1$  shrinks to 1. In the simulation with weight 2691, the window sizes of all sources  $S_1 \sim S_9$  shrink to 1 packet. In order to obtain larger weighted shares, the control loops must either send slower or the queue must grow. As we know from Figure 5(b), the queue does not grow for simulations with weights above 491. Instead, we use rate-based pacing to halve the send rate whenever the window size reaches 1 and the negative feedback arrives. When the positive feedback arrives we react in the same way as before.

This handling for the regime of low rates is similar to the exponential back-off used by TCP when a timeout occurs and the immediate recovery to a rate of one packet per RTT when an acknowledgement arrives. Jumping to one packet per RTT represents an aggressive increase that biases the weighted share in favor of the control loops with smaller weights. This aberration occurring at high weights might be solved through careful redesign of the increase step used in the low rate regime.

As shown in Figure 5(c), without AQM, the utilization is 100%. With AQM the utilization settles around 98%, which is our target utilization for AVD.

## C. Accumulation-based vs. Loss-based Approaches

The related research has explored how to modify TCP Reno's handling of packet loss to provide similar rate differentiation. In this subsection we compare the mechanisms used by the loss-based approach and in this paper. We argue that the accumulation-based approach is in principle better than the loss-based one in that the former can achieve a significantly larger range of service differentiation (as shown by the simulation results) and at the same time maintain good dynamic performance.

In [9] [25], the service is achieved by (adaptively) changing congestion control increase/decrease parameters. This approach creates a dilemma: it is hard to achieve *both* service differentiation and good dynamic performance because the increase/decrease parameters of the congestion control algorithm decide its dynamic performance. For example, larger increase/decrease parameters lead to larger oscillation of the congestion window. Large oscillation leads to burst losses and timeouts,

which is why [9] and [25] suffer. Further, packet loss can only be measured accurately over long periods of time, which accounts for their long simulation run-times.

Our accumulation-based approach achieves service differentiation by *moving the equilibrium* of the control algorithm in Equation (3). This *decoupling* of the steady state equilibrium and the dynamics of the control algorithm provides the capability to achieve the targeted service as well as good dynamic behavior (large weights without increased oscillation). So the better performance of Monaco results from the fact that accumulation is more manageable than loss for the purpose of service differentiation.

Of course, since we need to keep a steady state physical queue (i.e., accumulation) for each flow, and  $q_l$  is limited by the physical buffer size  $Q_l$  shown in the constraint (18), the bottleneck buffer size limits the range of the weighted service in practice. But this limitation is very different from that of [9] [25], which results from the coupling of the steady state objective and the dynamic performance.

## VI. SERVICE MULTIPLEXING

In this section we provide ns-2 simulation and Linux kernel implementation results to demonstrate that EMR and WRS can *co-exist dynamically* with bursty web-like traffic in a complex multiple-bottleneck network including both non-AQM droptail and AVD routers.

### A. Simulations

Firstly we show the simulation results for the network shown in Figure 6(a). We choose a topology with all equal capacities and put all control loops with EMRs along the multiple-bottleneck path, because these choices simplify target rate computations, which are described momentarily. There are four “long” flows passing through all the bottlenecks and a set of “cross” flows each using only one bottleneck. Every bottleneck link has 100Mbps capacity and 1ms propagation delay. The source nodes (1,0)~(1,3) are connected to  $R_0$  with propagation delays evenly spread between 1ms and 100ms, i.e., 1ms, 34ms, 67ms and 100ms, respectively. Nodes (2,0)~(2,3) have the same delays but are connected to  $R_1$  and likewise for nodes (3,0)~(3,3) to  $R_2$ . As specified in Table I, each of the long flows has an EMR, and they start and stop sending at different times thereby moving the system from undersubscribed through oversubscription and back to undersubscribed before a barrage of web-like flows start. The 500 web-like flows entering  $R_1$  are evenly distributed across

TABLE I  
MULTIPLE-BOTTLENECK SIMULATION PARAMETERS

flow	expected rate ( $x_{ije}$ )	A limit ( $A_{ij}$ )	weight ( $w_{ij}$ )	start time	stop time
(0,0)	30Mbps	60KB	1	$U[0, 5]$ s	
(0,1)	35Mbps	75KB	1	25s	75s
(0,2)	50Mbps	60KB	1	50s	75s
(0,3)	10Mbps	15KB	1	$U[0, 5]$ s	
(2,0)	0Mbps		3	$U[0, 5]$ s	
web	0Mbps		1	100s	
other	0Mbps		1	$U[0, 5]$ s	

twenty-five nodes, and each of these nodes is connected to  $R_1$  again with propagation delays evenly spread between 1ms and 100ms. The other twenty-five nodes generating web-like bursty traffic to  $R_2$  are similarly connected. We use Barford and Crovella’s web model [3], in which each user downloads a set of files representing a web page and then sleeps for a period of time. The requested file size and sleep times obey heavy-tailed distributions and thus the resulting traffic is quite bursty. In Figure 6(a), we show the web users entering at R1 and R2 while in fact this means that the bulk of the traffic they generate enters R1 and R2. Because clients download more data than they upload, this implies that the web servers are placed at R1 and R2 while their respective clients are attached to R2 and R3.

To determine the target rate allocation when there is no oversubscription, we subtract the EMRs from the capacities in each bottleneck and then compute the weighted proportional fair share. Let  $K$  denote the number of bottlenecks. Let  $M$  denote the sum of the number of control loops passing through all three bottlenecks and the number of cross-flows entering each bottleneck. Thus, the target rate allocation  $x_{ij}^*$  for the flow  $(i, j)$  is

$$x_{ij}^* = \begin{cases} \frac{w_{ij}}{W} C + x_{ije} & \text{if } i = 0 \\ \frac{w_{ij}}{W_i} (1 - \frac{W_0}{W}) C & \text{if } i \neq 0 \end{cases} \quad (28)$$

where  $C = 100 - \sum_{0 \leq j < M} x_{0je}$ ,  $W_i = \sum_{0 \leq j < M} w_{ij}$  and  $W = \sum_{0 \leq i < K} W_i$ .

If a control loop with an EMR  $x_{0je}$  incurs its accumulation limit, we simply set its EMR to zero and replace its weight with the control loop’s accumulation limit to compute its degraded service rate. We describe the following cases.

1) *No Oversubscription*: As specified in Table I, the long flows labeled (0,0) and (0,3) as well as all the cross flows that traverse a single bottleneck start at a uniformly distributed random time in  $0 \sim 5$ s, denoted as  $U[0, 5]$ s. The sum of the EMRs for (0,0) and (0,3) is 40Mbps, well below the bottleneck capacity. Neither flow needs

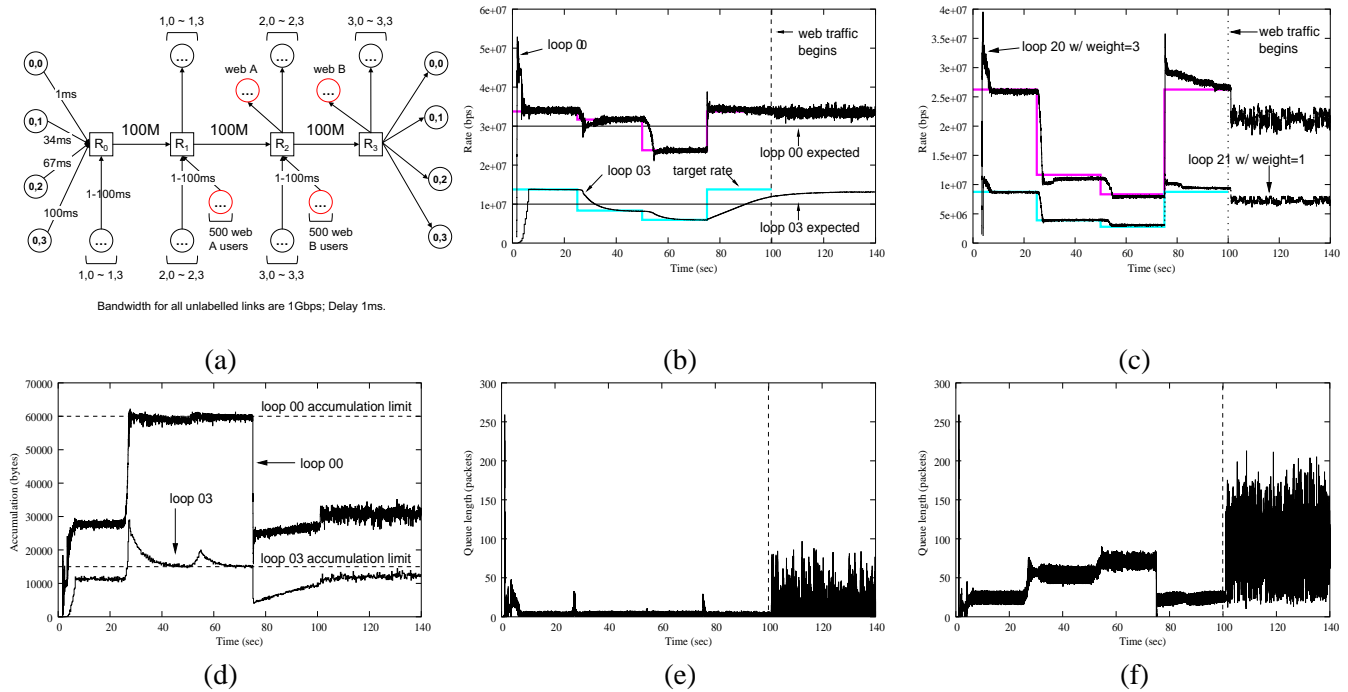


Fig. 6. Simulation of all services co-exist in a complex network of three bottlenecks: (a) A parking lot topology of 3 bottlenecks shared by the long and short flows, plus 1,000 web sessions; (b) EMR flow throughput: Flow (0,0) gets its expected 30Mbps bandwidth, except during 50~75s when its accumulation limit of 60KB takes effect; Flow (0,3) gets its expected 10Mbps bandwidth, except during 25~75s when its accumulation limit of 15KB takes effect; (c) WRS flow throughput: Flow (2,0) gets 3 times of bandwidth of flow (2,1); (d) Accumulation for flows with rate expectations. When the accumulation of an EMR flow touches its preset limit, its EMR degrades, as shown in (b); (e) AVD bottleneck  $R_1$  queue length is very low, even after the web traffic comes in; (f) Droptail bottleneck  $R_2$  queue length is proportional to the number of active flows. It is made more bursty by the web traffic during 100~140s. We set  $\kappa=0.5$ , target accumulation  $a_{ij}=3 * w_{ij}$ KB, AVD's damping factor  $\alpha=0.1$  and target utilization  $\beta=0.98$ .

to incur an accumulation greater than its accumulation limit to achieve its EMR. Thus, as shown in Figure 6(b), both flow (0,0) and (0,3)'s EMRs are satisfied and they obtain their respective target rates as determined by Equation (28).

2) *Accumulation-limited*: At 25s in the simulation, flow (0,1) begins transmitting and steers toward an EMR of 35Mbps. The sum of the active EMRs 75Mbps is still less than the capacity, but for flow (0,3) to achieve its expected rate would require  $a_{03} > A_{03}$ . Therefore, flow (0,3) becomes bounded by its accumulation limit shown in Figure 6(d) and fails to obtain its EMR. Even though  $x_{00e}$  and  $x_{01e}$  are larger than  $x_{03e}$ , they are satisfied because we have a policy of giving them larger accumulation limits.

3) *Oversubscription*: At 50s, flow (0,2) begins transmitting, resulting in blatant oversubscription. Because all of the EMRs are themselves less than the capacity, we would intuitively desire to have a subset of the EMRs satisfied. Unfortunately, flows (0,0), (0,1) and (0,2) all have similar accumulation limits thereby forcing all to a weighted proportionally fair share satisfying none of the EMRs, as shown in Figures 6(b) and (d). But none of

the flows without an expected rate are starved.

At 75s, flows (0,1) and (0,2) stop sending thereby allowing the system to return to an equilibrium that satisfies all expected rates for active flows. Throughout the simulation,  $x_{03}$  changes slowly compared to  $x_{00}$ , shown in Figure 6(b). This can be attributed to the large difference in round trip propagation delays: Flow (0,0) has 10ms while flow (0,3) has 208ms. However, despite their difference in propagation delays these flows still converge onto the appropriate target rate allocation throughout the simulation, or at least until the web-like traffic begins at 100s, at which time the equilibrium is no longer well-defined.

4) *Web-like Traffic*: At 100s, five hundred web users entering bottleneck  $R_1$  and five hundred web users entering bottleneck  $R_2$  introduce substantial variation in queue lengths, illustrated in Figures 6(e)-(f). We determined empirically an appropriate number of web users by turning off all sources except web users. We then tuned the number of web users to consume approximately 10% capacity. Of course, due to burstiness loads are sometimes much higher. The key result is that despite burstiness, each control loop hovers above its expected

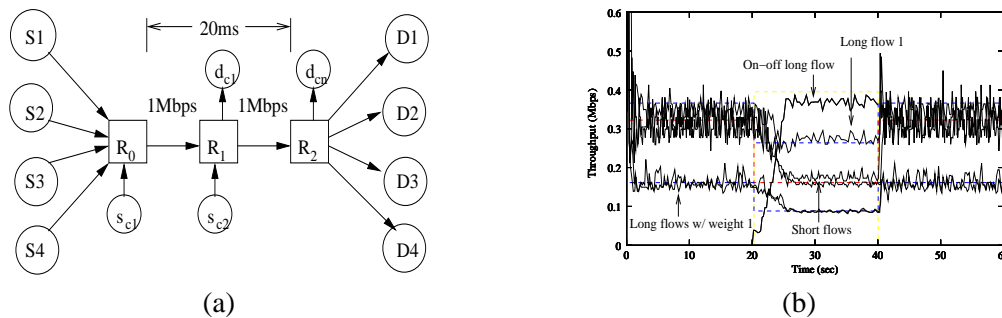


Fig. 7. Implementation results of all the services co-existing in a network of two bottlenecks: (a) Topology; (b) Each flow gets a throughput around its target value shown in the dashed lines.

rate shown in right side of Figure 6(b).

Again flow (0,3) appears to adjust more slowly than flow (0,0) (thus with less oscillation) in response to the bursty web traffic because of its much longer RTT, but it stays near the expected value.

5) *Coexisting Bottleneck Mechanisms: Droptail and AVD*: As shown in the topology Figure 6(a), bottleneck  $R_1$  uses AVD while others use droptail without AQM. Figures 6(e)-(f) readily demonstrate the benefits of AVD. The bottleneck  $R_1$  experiences equilibrium queue lengths near zero independent of the changing rate allocations. Even when the web traffic starts, its queue still remain substantially lower than that of  $R_2$ .

6) *Weighted Sharing*: Flow (2,0) sends with weight 3 throughout the experiment. For comparison we show its neighboring flow (2,1) with weight 1. Because these flows traverse the same path, we expect (2,0) to obtain roughly three times the throughput of (2,1) regardless of the changing rate expectations or the presence of web-like flows. Figure 6(c) reveals this. Furthermore, it shows that as the load from the EMR flows changes, each control loop steers toward the new rate allocation corresponding to proportional fairness for the capacity not allocated to the satisfied EMRs.

Showing Monaco EMR and WRS performance under different scenarios, the simulation results in this section demonstrate that all the proposed services can be provided in a dynamic environment with non-trivial bursty background traffic. The target rate allocations are well-defined and controllable via our choice of accumulation limits  $A_i$  even under oversubscription.

### B. Implementation Experiments

We also implement Monaco in Linux kernel v2.2.18 based on the Click configurable router [17] and perform a set of experiments on the Utah Emulab [20].

We show one result here for a two-bottleneck network shown in Figure 7(a) with 1Mbps link bandwidth and

20ms one-way delay. There are four long flows which pass all bottlenecks and two cross flows each using only one bottleneck. Long flow 1 asks for an EMR rate of 0.2Mbps. Long flow 2 requests a WRS service with weight 5. All other flows have weight 1. Long flow 2 is an on-off flow with a period of 20s. We did the experiment for 60s. As depicted in Figure 7(b), each flow gets its targeted rate.

Comparing to the previous simulations, implementation results oscillate more. This comes mainly from the limited timer granularity in Linux kernel which makes traffic less regulated (more bursty) than in ns-2.

## VII. DISCUSSION

We focus on using closed-loop congestion control mechanisms as a data plane building block to provide better QoS than the Internet's best-effort service. Both TCP Vegas and Monaco are delay-based, while TCP Reno is loss-based. All of them are close-loop congestion control schemes. For congestion control purpose, we compared Monaco and Vegas in a previous paper [31]. The central theme of this paper is that, within the close-loop schemes, accumulation is a more manageable parameter in providing service differentiation than loss, as shown in our analysis and simulations.

There are several important deployment issues for our scheme. The first concern is scalability. Monaco requires each (congested) router to provide two FIFO priority queues for all EMR and WRS flows. Since these are not per-flow queues, scalability along this dimension is not a problem.

The overhead of the Monaco control traffic is very low. For each flow, there are only three control packets, one in-band and the other two out-of-band, *per RTT*. The control packets are small (40 bytes). Consider a typical situation of a flow with an average congestion window of ten packets and each data packet is 1000 bytes, the control packets overhead is about  $\frac{3 \times 40}{10 \times 1000} \approx 1.2\%$ . Furthermore, when integrated with TCP, Monaco can

use existing TCP packets to carry the IB and OB control packet information and would thus introduce no separate traffic.

Compared to DiffServ which places all its data plane building blocks inside the network, Monaco moves some complexity from the core network to network edges or even end hosts. Albeit, Monaco still needs network support, such as two FIFO queues and AVD for routers with underprovisioned buffer. Note AVD routers can interoperate with non-AQM droptail routers (see Section IV-A). This makes Monaco more incrementally deployable.

One interesting scenario is to deploy Monaco in an edge-to-edge manner. Then an ISP can provide EMR or WRS traffic trunks to carry its customers' flow aggregates across its network boundaries.

### VIII. SUMMARY

In this paper we propose an accumulation-based, closed-loop congestion control mechanism to provide bandwidth differentiation and guarantees, based on our prior work of using accumulation, buffered packets of a flow inside the network routers as a measure to detect and control network congestion. The key idea is to map service provisioning onto accumulation allocation. We design two concrete services: EMR and WRS. Analytically as well as experimentally, we show that accumulation can be appropriately manipulated to provide each specific service. Because of the use of the closed-loop congestion control, these bandwidth services are meaningful only in the steady state, at the flow (not packet) granularity and in a time scale that is larger than one RTT.

We use a set of ns-2 simulations to evaluate the service performance under different network topologies and conditions. We demonstrate that both services can be provided in a network with dynamic demands, under the conditions of oversubscription and router buffer limits. We implement the scheme in the Linux kernel based on the Click router and validate the simulation results using the Utah Emulab and an internal testbed.

This paper focuses on the data-plane building blocks for the service provisioning. The related control plane functions and architectural issues, such as the mapping of the scheme in an edge-to-edge manner to provide cross-ISP services, represent our future research.

### IX. ACKNOWLEDGMENTS

The authors would like to thank Josh Hort, Kishore Ramachandran and Rahul Sachdev for performing ns-2 simulations. They are grateful for the insightful comments from the anonymous reviewers. This work was

supported in part by the NSF contracts ANI-9806660 and ANI-9819112, by the DARPA contract F30602-00-2-0537, and a grant from Intel Corp.

### REFERENCES

- [1] S. Athuraliya, V. Li, S. Low and Q. Yin. REM: Active Queue Management. *IEEE Network*, 15(3):48-53, May 2001.
- [2] ATM Forum. [Http://www.atmforum.com/](http://www.atmforum.com/).
- [3] P. Barford and M. Crovella. A Performance Evaluation of Hyper Text Transfer Protocols. *SIGMETRICS'99*, Mar 1999.
- [4] S. Blake et al. An Architecture for Differentiated Services. *IETF RFC 2475*, Dec 1998.
- [5] R. Braden, D. Clark, and S. Shenker. Integrated Services in the Internet Architecture: an Overview. *IETF RFC 1633*, Jun 1994.
- [6] L. Brakmo and L. Peterson. TCP Vegas: End to End Congestion Avoidance on a Global Internet. *IEEE Journal on Selected Areas in Communications*, 13(8):1465-1480, Oct 1995.
- [7] D. Choe and S. Low. Stabilized Vegas. *INFOCOM'03*, Apr 2003.
- [8] D. Clark and W. Fang, Explicit Allocation of Best Effort Packet Delivery Service. *IEEE/ACM Trans. on Networking*, 6(4):362-373, Aug 1998.
- [9] J. Crowcroft and P. Oechslin. Differentiated End-to-End Internet Services Using a Weighted Proportional Fair Sharing TCP. *ACM Computer Communication Review*, 28(3), Jul 1998.
- [10] A. Demers, S. Keshav, and S. Shenker. Analysis and Simulation of a Fair Queueing Algorithm. *SIGCOMM'89*, Sept 1989.
- [11] S. Floyd and V. Jacobson. Random Early Detection Gateways for Congestion Avoidance. *IEEE/ACM Trans. on Networking*, 1(4):397-413, Aug 1993.
- [12] Frame Relay Forum. [Http://http://www.frforum.com/](http://http://www.frforum.com/).
- [13] D. Harrison. Edge-to-edge Control: A Congestion Avoidance and Service Differentiation Architecture. *RPI Ph.D. Thesis*, Dec 2001. [Http://networks.ecse.rpi.edu/~harrisod/thesis.ps.gz](http://networks.ecse.rpi.edu/~harrisod/thesis.ps.gz).
- [14] H. Hsieh, K. Kim and R. Sivakumar. Achieving Weighted Service Differentiation: An End-to-End Perspective. *IwQoS'03*, Jun 2003.
- [15] V. Jacobson. Congestion Avoidance and Control. *SIGCOMM'88*, Aug 1988.
- [16] F. Kelly, A. Maulloo and D. Tan. Rate Control in Communication Networks: Shadow Prices, Proportional Fairness and Stability. *Journal of the Operational Research Society*, 49:237-252, 1998.
- [17] E. Kohler, R. Morris, B. Chen, J. Jannotti, and F. Kaashoek. The Click Modular Router. *ACM Trans. on Computer Systems* 18(3):263-297, Aug 2000.
- [18] S. Kunniyur and R. Srikant. End-To-End Congestion Control: Utility Functions, Random Losses and ECN Marks. *INFOCOM'00*, Mar 2000.
- [19] S. Kunniyur and R. Srikant. Analysis and Design of an Adaptive Virtual Queue (AVQ) Algorithm for Active Queue Management. *SIGCOMM'01*, Aug 2001.
- [20] J. Lepreau et al. The Utah Emulab. [Http://www.emulab.net/](http://www.emulab.net/).
- [21] S. Low and D. Lapsley. Optimization Flow Control, I: Basic Algorithm and Convergence. *IEEE/ACM Trans. on Networking*, 7(6):861-875, Dec 1999.
- [22] S. Low, L. Peterson and L. Wang. Understanding TCP Vegas: A Duality Model. *SIGMETRICS'01*, Jun 2001.
- [23] L. Massoulié and J. Roberts. Bandwidth Sharing: Objectives and Algorithms. *INFOCOM'99*, Mar 1999.
- [24] J. Mo and J. Walrand. Fair End-to-End Window-based Congestion Control. *IEEE/ACM Trans. on Networking*, 8(5):556-567, Oct 2000.

- [25] T. Nandagopal et al. Scalable Service Differentiation using Purely End-to-End Mechanisms: Features and Limitations. *IPQoS'00*, Jun 2000.
- [26] Network Simulator ns-2. [Http://www.isi.edu/nsnam/ns/](http://www.isi.edu/nsnam/ns/).
- [27] A. Parekh and R. Gallager. A Generalized Processor Sharing Approach to Flow Control in Integrated Services Networks: The Single-Node Case. *IEEE/ACM Trans. on Networking*, 1(3):344–357, Jun 1993.
- [28] K. Ramakrishnan and S. Floyd. A Proposal to Add Explicit Congestion Notification (ECN) to IP. *IETF RFC 2481*, Jan 1999.
- [29] I. Stoica. Stateless Core: A Scalable Approach for Quality of Service in the Internet. *CMU Ph.D. Thesis*, Dec 2000.
- [30] Z. Wang. User-Share Differentiation (USD): Scalable Bandwidth Allocation for Differentiated Services. *IETF Draft*, Nov 1997.
- [31] Y. Xia, D. Harrison, S. Kalyanaraman, K. Ramachandran, and A. Venkatesan. Accumulation-based Congestion Control. *Accepted by IEEE/ACM Transactions on Networking*, Feb 2004. [Http://www.rpi.edu/~xiay/pub/acc.ps.gz](http://www.rpi.edu/~xiay/pub/acc.ps.gz).